Original Article

Journal of Tissue Engineering
Volume 6: 1–11
© The Author(s) 2015
DOI: 10.1177/2041731415592075
tej.sagepub.com
SAGE

Vertical osteoconductivity of sputtered hydroxyapatite-coated mini titanium implants after dura mater elevation: Rabbit calvarial model

Xin Wang[1], Osama Zakaria[1,2], Marwa Madi[3] and Shohei Kasugai[1]

Abstract

This study evaluated the quantity and quality of newly formed vertical bone induced by sputtered hydroxyapatite-coated titanium implants compared with sandblasted acid-etched implants after dura mater elevation. Hydroxyapatite-coated and non-coated implants (n = 20/group) were used and divided equally into two groups. All implants were randomly placed into rabbit calvarial bone (four implants for each animal) emerging from the inferior cortical layer, displacing the dura mater 3 mm below the original bone. Animals were sacrificed at 4 (n = 5) and 8 (n = 5) weeks post-surgery. Vertical bone height and area were analyzed histologically and radiographically below the original bone. Vertical bone formation was observed in both groups. At 4 and 8 weeks, vertical bone height reached a significantly higher level in the hydroxyapatite compared with the non-coated group ($p < 0.05$). Vertical bone area was significantly larger in the hydroxyapatite compared with the non-coated group at 4 and 8 weeks ($p < 0.05$). This study indicates that vertical bone formation can be induced by dura mater elevation and sputtered hydroxyapatite coating can enhance vertical bone formation.

Keywords

Vertical osteoconductivity, dura mater, sputter coating, hydroxyapatite coating, implants

Received: 8 March 2015; accepted: 21 May 2015

Introduction

Vertical bone augmentation remains a considerable problem. Although several reconstruction procedures have been proposed, autogenous bone grafting is still regarded as the gold standard.[1] However, resorption of bone grafts after vertical bone augmentation is the main concern for clinicians.[2,3]

Using the body's own ability to induce bone formation is a recent regeneration trend that depends on harnessing the intrinsic regenerative potential of endogenous tissues, avoiding *ex vivo* culture of autologous cells and the requirement for synthesized scaffolds. This approach suggests an alternative to traditional tissue engineering modalities for bone augmentation.[4] In a series of publications, Zakaria et al.[1,5,6] reported that bone augmentation was achieved using a periosteal distractor through creation of a sizeable secluded supraosteal regenerative space. Kammerer et al.[7] and Schiegnitz et al.[8] also demonstrated that vertical bone formation was successfully guided by calcium-phosphate-coated or "sandblasted, large-grit, acid-etched (SLA)" surface implants in a subperiosteal rabbit model without

[1]Department of Oral Implantology and Regenerative Dental Medicine, Tokyo Medical and Dental University, Tokyo, Japan
[2]Department of Oral and Maxillofacial Surgery, Pharos University in Alexandria, Alexandria, Egypt
[3]Department of Oral Medicine, Periodontology, Oral Diagnosis and Radiology, Faculty of Dentistry, Alexandria University, Alexandria, Egypt

Corresponding author:
Xin Wang, Department of Oral Implantology and Regenerative Dental Medicine, Tokyo Medical and Dental University, 1-5-45 Yushima, Bunkyo-ku, Tokyo 113-8510, Japan.
Email: wangirm@tmd.ac.jp

assistance of any growth factors or bone substitutes. Additionally, spontaneous bone formation after creation of a secluded space between the bone surface and sinus membrane has been demonstrated in numerous animal and clinical studies, which suggests that displacing the maxillary sinus lining results in new bone (NB) formation around the protruded part of the implant.[9–12]

The dura mater is the tissue that exists between the calvarial bone and brain and functions primarily as a protective covering of the brain. It is composed of two layers, the endosteal and meningeal.[13] Populated by nerves and blood vessels, the outer endosteal layer serves as the periosteum and is thought to be a source of osteoprogenitors in the calvaria that contribute to bone healing initiation,[3,14–18] while the inner meningeal layer forms the cerebral falx, sellar diaphragm, and tentorium.[13,19,20] Previous studies have demonstrated that the dura mater retains the capacity to form bone or bone nodules in calvarial defects.[3,21] In animal studies in which the dura mater was resected together with the overlying calvarial bone, or excluded by a polytetrafluoroethylene membrane, the defect was replaced by fibrous tissue with no bone island formation or significantly less bone formation.[3,22] In an *in vitro* study, the dura mater has been found to express significantly greater amounts of bone morphogenetic protein (BMP)-2, BMP-4, and BMP-7 to facilitate bone regeneration.[23] Importantly, maintenance of dural integrity is also essential for complete bone regeneration.[24–26]

Hydroxyapatite (HA) is a promising biomaterial with potential bioactivity and osteoinductivity properties.[8] Currently, HA is used mainly as a coating for dental implants to improve surface characteristics, thus converting titanium surfaces into bioactive ones with high bone-bonding properties.[8,27] A number of methods have been developed to deposit HA coating, with plasma spraying being the most common technique, which resulted in a thick coated layer (50 μm in average) onto the titanium surface.[28] However, disadvantages of this technique include nonuniformity of the coating density, micro-cracks on the coating surface, and poor resistance to delamination.[29,30] More recently, the coating technique has been greatly improved and sputtered HA coating is a novel coating technique that can produce an ultra-thin layer of HA coating (1-μm thickness) onto the substrates with strong adhesion, a compact microstructure, and preservation of the surface roughness of the underlying substrate.[31–34] In an *in vivo* study, osseointegration was rapidly enhanced using the sputtered HA-coated implants compared with non-coated (NC) implants.[35] Similarly, an *in vitro* study reported that osteoblastic differentiation was significantly enhanced on sputtered HA-coated samples compared with NC samples.[33]

In this study, to evaluate the osteogenic capacity of the dura mater, HA-coated and NC implants were used to elevate the dura mater. It was hypothesized that the vertical bone induced around the implants after dura mater elevation, and the amount of bone formation, could be significantly enhanced around sputtered HA-coated implants. In addition, the suitability of this rabbit calvaria model in testing implant surface characteristics was also evaluated.

Materials and methods

Sample preparation

Forty commercially pure titanium Osteosynthesis Screws (Yamahachi Dental Manufacturing Company, Tokyo, Japan) with a length of 6.0 mm and a diameter of 2.0 mm were used in this study as a model of mini dental implants. Sputtered HA coating was carried out according to the description in previous studies.[36,37] In brief, all implants were subjected to sandblasting by apatite grids in the range of 180–1180 μm, followed by acid-etching treatment in hydrochloric acid solution (6 N) for 5 min at room temperature.[33] Then, radio frequency magnetron sputtering was performed on 20 implants using an SPF-410H chamber (Anelva Corp., Tokyo, Japan.) to produce an HA coating with an average thickness of 1.1 μm. Subsequently, hydrothermal treatment was carried out at a temperature of 110°C in an electrolyte solution containing calcium and phosphate ions for 24 h.[36] Finally, two titanium surface treatments were produced for this experiment: (a) 20 implants with sandblasted, acid-etched surfaces serving as a control group (NC group) and (b) 20 implants with a 1-μm-thick HA coating on the surfaces as a test group (HA-coated, HA group).

Animal care and surgical procedures

The experimental protocol was approved by the Committee of Animal Experiments at Tokyo Medical and Dental University, Tokyo, Japan. Ten, 6-week-old Japanese male rabbits (Saitama Experimental Animals Supply, Kyoto, Japan) weighing from 2.5 to 3 kg were included in the study.

An intramuscular injection of ketamine (50 mg/kg Ketalar; Ankyo, Tokyo, Japan) and thiopental sodium (25 mg/kg Rabonal; Tanabe, Tokyo, Japan) was used to anesthetize all animals preoperatively. Additionally, local anesthetic (2% xylocaine/epinephrine 1:80,000; 1.8 mL; Dentsply Sankin, Tokyo, Japan) was injected around the surgical areas before the start of surgery.

All surgical procedures were carried out under aseptic conditions. The surgical areas were shaved and scrubbed with a tincture of 1% iodine solution. For each animal, midline skin and subperiosteal incisions were performed over the calvarial bone from the orbits to the external occipital protuberance. The skin and periosteal flap were meticulously raised up and bilaterally retracted to expose the bone surface. Two groups were established and designed as

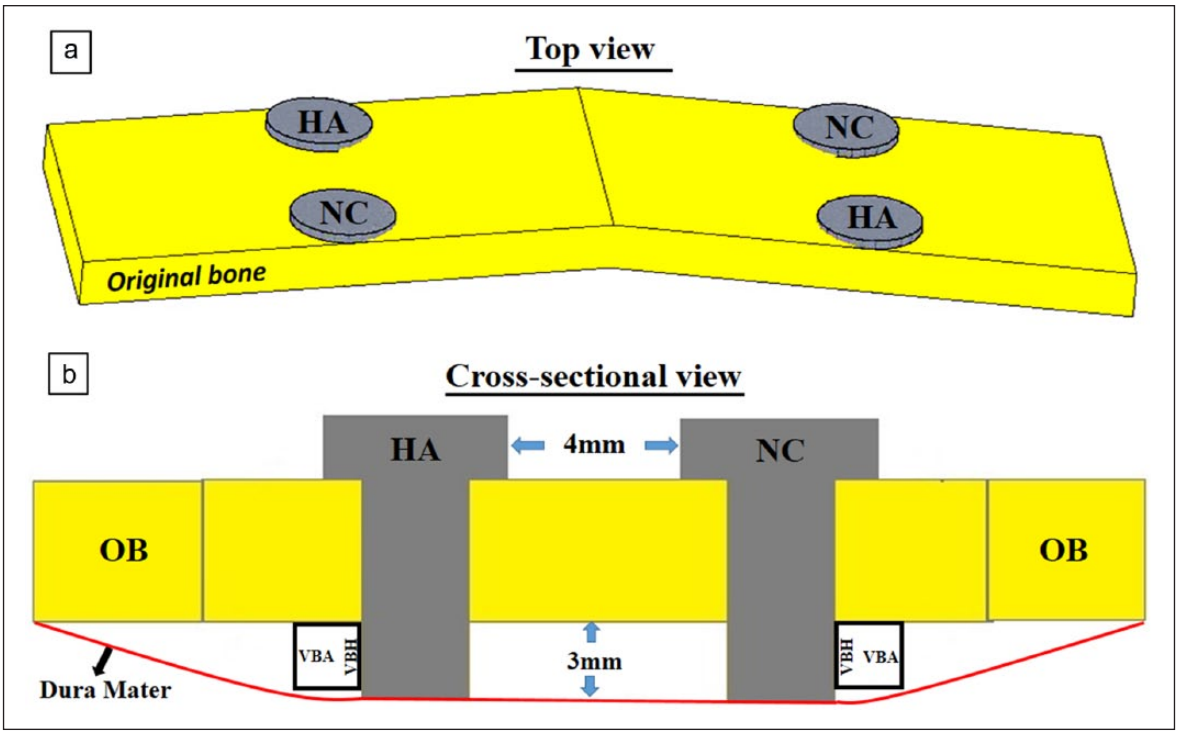

Figure 1. Schema of implant placement and determined parameters: (a) for each calvarium, four implants (two HA-coated and two non-coated) were placed beside the mid-line of the original bone (OB) from the top view; (b) all implants were placed 3 mm below the OB and the distance in between each implant was set at 4 mm.
VBH: vertical bone height; VBA: vertical bone area, newly formed bone area below the OB within a 3 × 3 mm^2 region of interest.

follows: (1) HA-coated implant and (2) NC implant for each calvarium. Under constant saline irrigation, two perforations, 1.8 mm in diameter and approximately 1.0 mm in depth, were drilled with a round bur in one side by the mid-line with a custom perforation template and repeated symmetrically for the other side. All perforations were then expanded 2.0 mm before implant placement. The two types of implants were randomly placed in their positions in the calvaria of all animals as shown in Figure 1(a). Following this, the periosteum was closed over the implants and the skin flap was sutured with 4-0 sutures (Ethicon, Somerville, NJ, USA). Finally, all implants were placed 3 mm extending from the inferior surface of calvarial bone displacing the dura meter downward as shown in Figure 1(b).

Physico-chemical characterization of implants

The morphologies of the two implant surfaces were observed using scanning electron microscopy (SEM) (JSM-5310LV; JEOL, Tokyo, Japan) at 15 kV. The X-ray diffraction (XRD) pattern was identified by RINT1400 (Rigaku Corp., Tokyo, Japan) using a CuKα radiation source operating at 50 kV and 100 mA excitation current. Implant surface roughness was calculated by a surface measurement tester (Surfcom 130A; Accretech Tokyo, Japan). Elemental analysis of the two implant surfaces was carried out by energy-dispersive X-ray spectroscopy (EDS) (EMAX-7000; Horiba Ltd, Kyoto, Japan) with a voltage of 15 kV for 100 s in a vacuum condition without conductive coating. The HA coating Ca/P molar ratio was further analyzed by EDS with carbon coating. All data were calibrated by PRZ Standard-less Quantitative Correction of the EMAX-7000 program (Horiba Ltd)

Ca/P molar ratio from original and newly formed bone by EDS

Injection of an excessive amount of ketamine (Ketalar; Ankyo) was used as the method to sacrifice the animals at 4 and 8 weeks after surgery. Following this, specimens were dissected out from the surgical area and immediately fixed in 10% neutralized formalin (Wako Chemical Co. Ltd, Tokyo, Japan) for 2 weeks. Subsequently, a high-resolution micro-computed tomography (CT) imaging system (SMX-90 CT; Shimadzu, Kyoto, Japan) was used to scan all specimens with a tube voltage of 90 kV and tube current of 110 μA. Then, all the scanned images were analyzed using three-dimensional image analysis software (TRI/3D-BON; Ratoc System Engineering, Kyoto, Japan).

The calcium (Ca) to phosphate (P) concentration was determined for all specimens by EDS including sections of original bone (OB) and the newly formed bone (15 kV

accelerating voltage for 100 original bone s in the vacuum condition with carbon coating). At each region, three equally distributed points were chosen, and then the mean values were calculated, respectively. All the data were calibrated by the PRZ Standard-less Quantitative Correction of the EMAX-7000 program (Horiba Ltd).

Histomorphometric analysis

Histological processing is described in detail in a previous study.[37] Briefly, all specimens were immersed in 10% formalin neutral buffer solution (Wako Chemical Co. Ltd) for 2 weeks. After complete fixation, all samples were rinsed for 3 h with tap water and then dehydrated in ascending grades of ethanol and afterward embedded in polyester resin (Technovit 7100; Heraeus Kulzer, Hanau, Germany). The implants were kept in place and each block was cut in a sagittal plane passing through the center of each implant using a commercial water-cooled saw (Exakt, Mesmer, Ost Einbeck, Germany). For each implant site, all were cut along the same cutting line and thinned out to a thickness of approximately 100 µm. The sections were finally stained with 0.1% toluidine blue. Histologic observation was carried out under a light microscope using a Leica DM8000 M microscope (Leica Microsystems, Heidelberg, Germany). The digitalized images were evaluated histomorphometrically using Image J software (Version 1.47v; NIH, Bethesda, MD, USA) to calculate the newly formed bone area and bone height.

Vertical bone height. Measurements (mm) were performed from the top of the newly formed vertical bone to the surface of the OB using Image J software (Version 1.47v; NIH) (Figure 1(b)). Vertical bone height (VBH) was defined as the newly formed bone height below the OB. All the mean ± standard deviation (SD) values were calculated for each sample.

Vertical bone area. Measurements (mm^2) were performed within a $3 \times 3\,mm^2$ region of interest at the lateral side of each implant below the OB surface using Image J software (Version 1.47v; NIH) (Figure 1(b)). Vertical bone area (VBA) was defined as the newly formed bone area below the OB within the region of interest (Figure 1). All the mean ± SD values were calculated for each sample.

Vertical NB–implant contact observation. Osseointegration at the interface between newly formed vertical bone and the implant surface of all samples was determined by histological evaluation as well as SEM observation (JSM-5310LV; JEOL) at 15 kV.

Statistical analysis

Statistical analysis was performed using IBM SPSS Statistics version 19.0 for Windows (IBM, Armonk, NY, USA). For all parameters, the mean and SD values were examined. Due to the low sample size in this study, descriptive *p*-values were only reported for all groups. The level of significance was set at $p < 0.05$.

Results

Experimental animals

All animals showed normal behavior in their cages after cessation of the general anesthesia effect. No animals died and no infections were detected during the entire period of the experiment. For all implant sites, the surgical areas did not exhibit any signs of inflammation and implants remained rigidly fixed to the calvaria during the experiment. All implants were completely covered by the skin at the time of killing. Noticeably, all animals gained an average weight of 0.22 kg during the observation intervals.

Physico-chemical characterization of HA coating

Implant surface morphology was observed by SEM. At low magnification (100×), HA-coated and NC surfaces showed similar microscale roughness (Figure 2(a) and (c)). At high magnification (3500×), crystalized HA particles were observed with a homogeneous distribution and compact form on the surface of the HA-coated implant, whereas a network of pits was detected on the surface of the NC implant (Figure 2(b) and (d)). The dotted and solid lines shown in the XRD pattern (Figure 3(a)) indicate the peaks of Ti and crystalized HA, respectively. EDS analysis confirmed that both implants were primarily composed of titanium and the presence of calcium and phosphate ions was only observed in the HA-coated implants (Figure 3(b) and (c)). The roughness (Ra) values of the NC and HA-coated implants were 1.25 ± 0.26 and 1.13 ± 0.39 µm, respectively (Table 1). The Ca/P molar ratio was measured for the HA-coated samples to ensure that the coating was as biologically similar as possible, whereby a Ca/P molar ratio of 1.70 ± 0.13 was achieved (Table 1) in line with a previous study.[36]

Observation of bone formation

Histological and micro-CT observation demonstrated that the space, which was raised up below the OB by the two implants, was almost completely occupied by newly formed bone that crept into the implant serrations, starting from the OB down to the end of the implant (Figure 4). This is an indication that significant bone formation was acquired below the OB after elevation of the dura mater. In addition, connective tissue was rarely detected in this region and histological images were almost similar at the two time points (4 and 8 weeks). Interestingly, a considerable amount of NB formation was also observed at the interproximal space in between the two implants below the

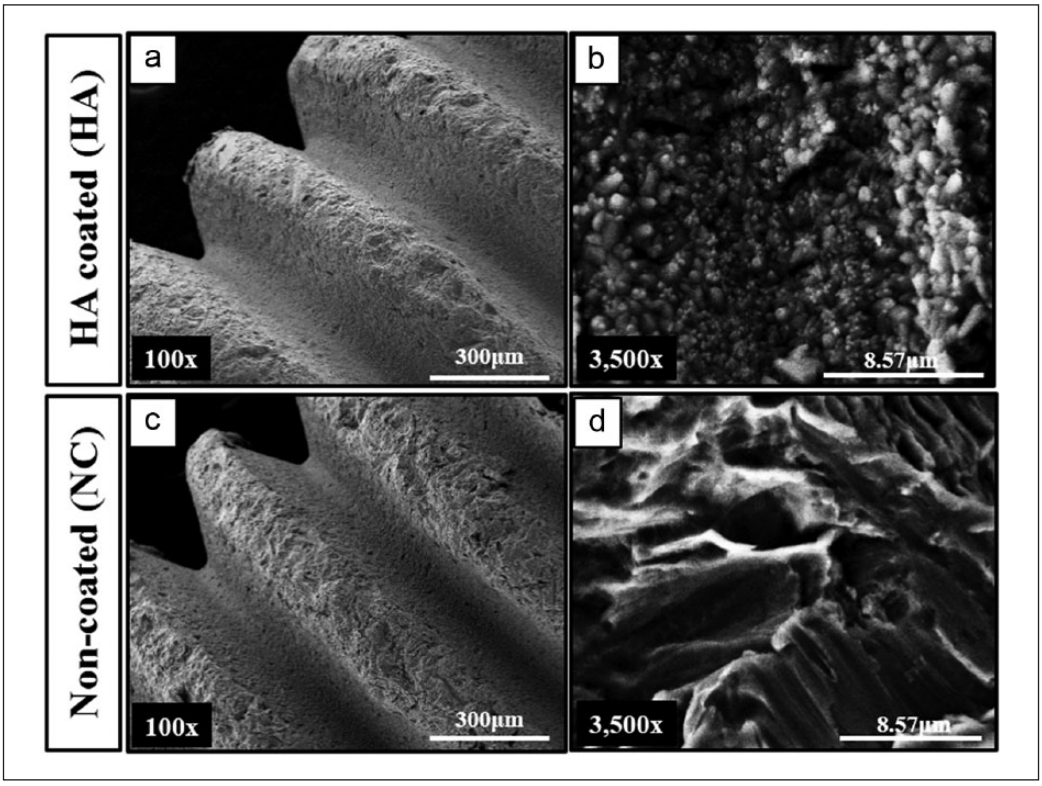

Figure 2. Scanning electron micrograph (SEM) images for HA-coated and non-coated implants: (a and c) at 100× magnification, a similar microscale was found between the HA-coated and non-coated implants, scale bar = 300 µm; (b and d) at 3500× magnification, homogeneous distribution of HA particles was observed on the surface of the HA-coated implant, whereas no HA particles were found on the non-coated implant surface, scale bar = 8.57 µm.

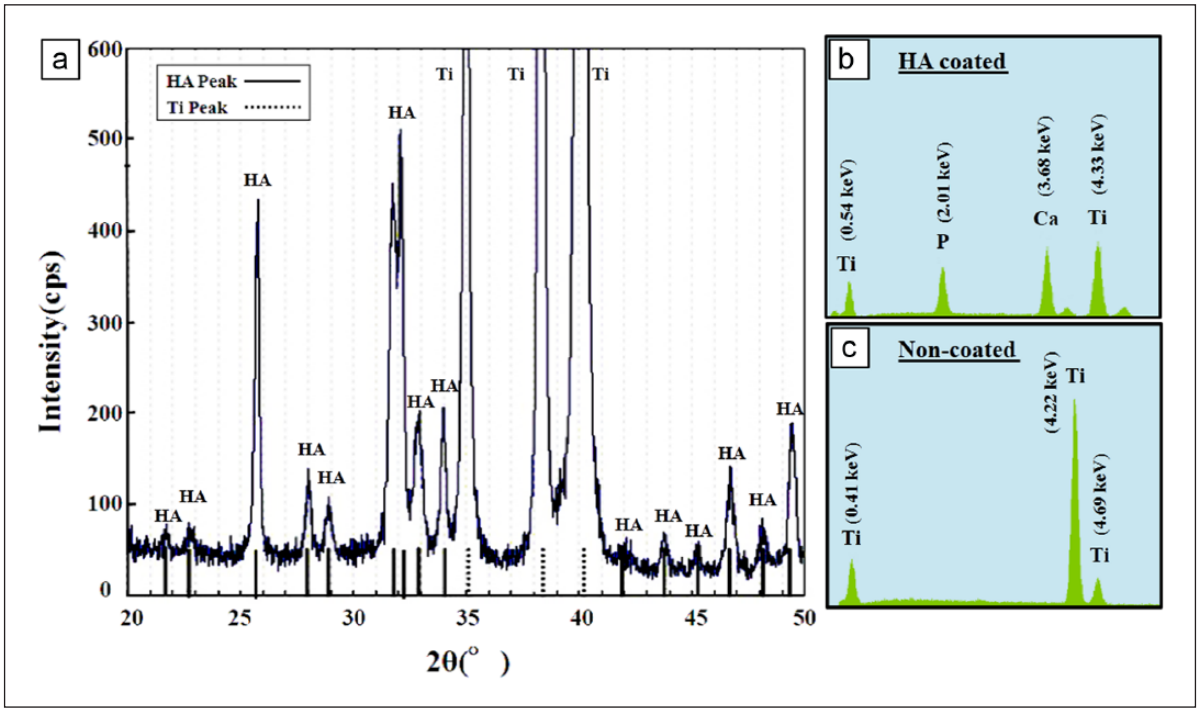

Figure 3. (a) X-ray diffraction pattern of the sputtered HA-coated implant. Energy-dispersive X-ray spectroscopy spectrum of the sputtered (b) HA-coated and (c) non-coated implants.

OB connecting the two implants together with structural and functional contact (Figure 4).

Looking closer, profound bone formation was observed around the implant within the space created below the OB in both groups (Figure 5). NB trabeculae were observed to creep onto the serration of the implants in an inclined pattern originating from the OB surface and covered by the layer of dura mater (Figure 5). NB was distinguished from OB by its comparatively thin trabeculae and darker staining (Figure 5).

The Ca/P molar ratio data for the newly formed vertical bone and OB are presented in Table 2. The Ca/P ratio range was from 1.73 ± 0.17 to 1.94 ± 0.06 and significant differences were not observed between groups.

Quantitative evaluation of bone formation

VBH below the OB. The height of newly formed vertical bone (VBH) below the OB was measured for both groups. At 4 weeks, the VBH had a mean of 1.57 ± 0.06 mm for the HA group and a mean of 1.01 ± 0.05 mm for the NC group. At 8 weeks, the mean value was 1.58 ± 0.30 mm for the HA group and 0.9 ± 0.17 mm for the NC group. VBH of the HA group was significantly higher when compared with the NC group at 4 and 8 weeks ($p < 0.05$) (Figure 6(a)).

Table 1. Surface roughness and Ca/P molar ratio (n = 16).

Sample	Ra (μm)	Ca/P
HA-coated	1.13 ± 0.39	1.70 ± 0.13
Non-coated	1.25 ± 0.26	Null

HA: hydroxyapatite.

VBA below the OB. In all groups, the space created below the OB was filled with cascade-like NB. VBA was measured for all samples in both groups. At 4 weeks, the mean VBA was 2.53 ± 0.26 and 1.65 ± 0.19 mm^2 for the HA and NC groups, respectively. At 8 weeks, the mean VBA was 2.21 ± 0.34 and 1.18 ± 0.21 mm^2 for the HA and NC groups, respectively. The VBA of the HA group was significantly larger when compared with the NC group at both 4 and 8 weeks ($p < 0.05$) (Figure 6(b)).

Vertical NB–implant contact

The bone–implant contact between the newly formed vertical bone and implant surface was evaluated histologically and by SEM. Remnant HA coating was observed by SEM on the HA-coated implants after 4 and 8 weeks. As shown in Figure 7, cascade-like newly formed bone was observed along the contour of the implant surface and bony ingrowth into the serrations was clearly detected in both implant surfaces. An intimate contact between the coating and the NB interface presented on the HA-coated implants exhibited tight osseointegration and strong chemical bonding. However, a noticeable micro-gap region between the implant surface and NB was frequently observed in the NC group (Figure 7).

Discussion

More recently, the positive function of the dura mater in the regeneration of calvarial defects has gained considerable attention.[3,18,22] Furthermore, it has been confirmed that the dura mater is more osteogenic than the periosteum in both infant and adult animals.[3] However, to our knowledge, data

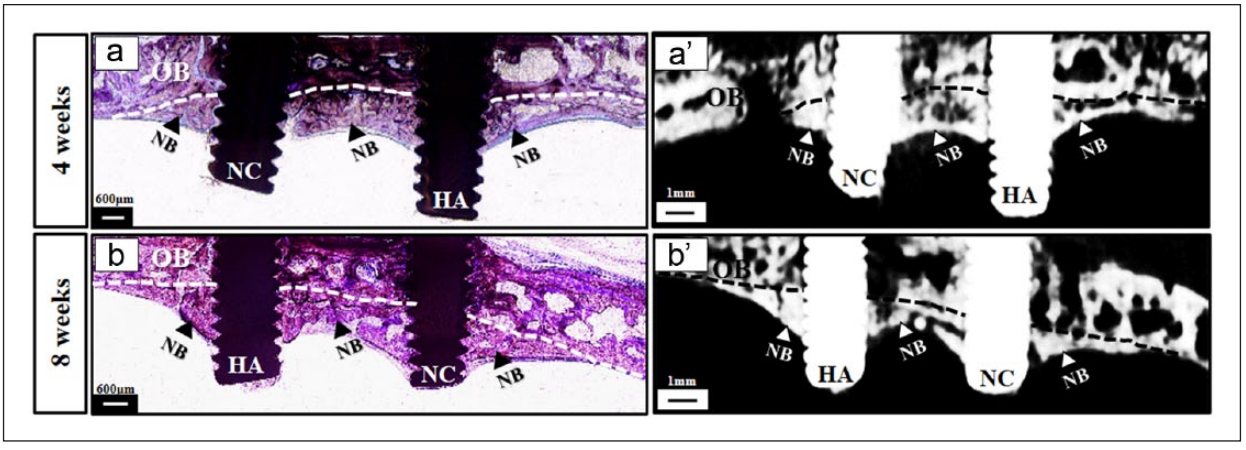

Figure 4. General observation of the newly formed bone induced by the implants after dura mater elevation. Comprehensively, new bone formation was observed below the original bone within the space raised up by the two implants and bone formation seemed to be consistent at 4 and 8 weeks. Note that a considerable amount of bone formation was in between the two implants (arrows) connecting the two implants together. (a and a′) Bone formation below the calvarial bone at 4 weeks; (b and b′) bone formation below the calvarial bone at 8 weeks.
HA: HA-coated implant; NC: non-coated implant; NB: newly formed bone; OB: original bone (outlined by dotted lines); scale bar in histological images = 600 μm; scale bar in micro-CT images = 1 mm.

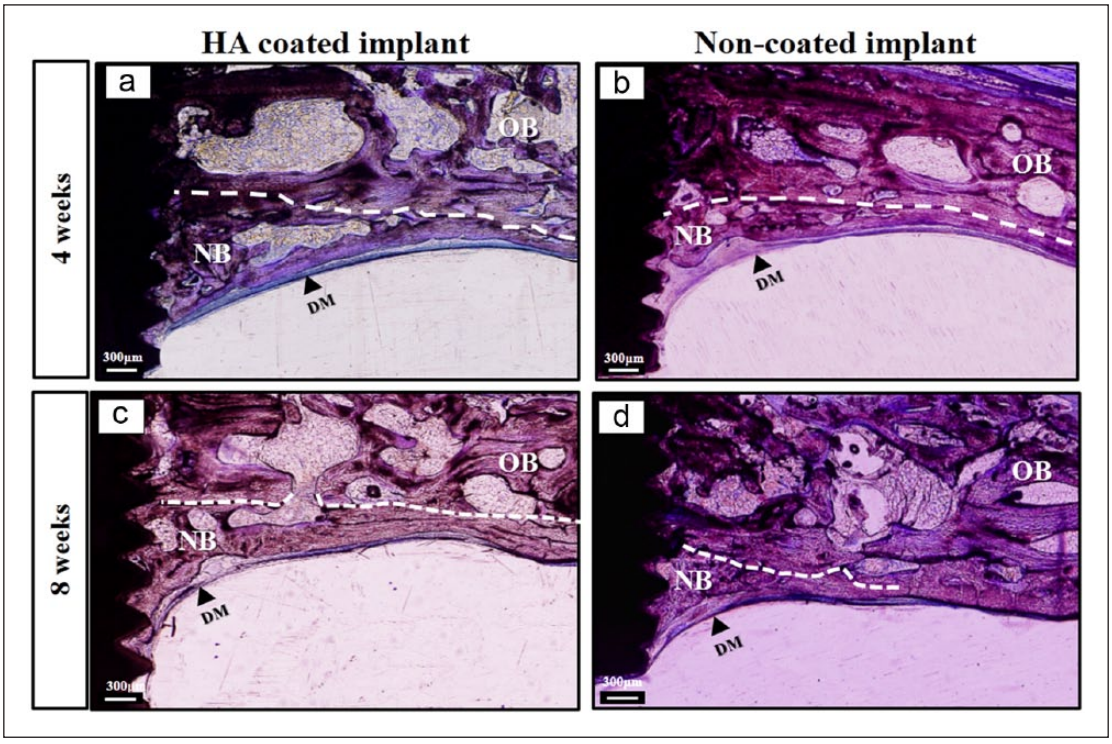

Figure 5. Vertical bone augmentation around implants in all groups at 4 and 8 weeks. New bone (NB) formation around implants was induced successfully after elevation of the dura mater in both groups at 4 and 8 weeks; the distinction was fairly consistent in terms of bone quantity among groups. Below the original bone, new bone trabeculae seemed to be significantly thicker in the HA-coated implant group compared to the non-coated implant group. (a and c) HA-coated implant and (b and d) non-coated implant. OB: original bone (outlined by white dotted lines); NB: newly formed bone; DM: dura mater; scale bar = 300 μm.

Table 2. Ca/P molar ratio from the new bone and original bone measured by (EDS).

	Ca/P molar ratio		
	OB	HA	NC
4 weeks	1.75 ± 0.15	1.79 ± 0.16	1.73 ± 0.17
8 weeks	1.90 ± 0.01	1.94 ± 0.06	1.85 ± 0.09

EDS: energy-dispersive X-ray spectroscopy; OB: original bone; HA: new bone below the original bone in HA group; NC: new bone below the original bone in NC group.

regarding the potential capacity to induce vertical bone formation after elevation of the dura mater have not been reported previously. In this study, newly formed bone below the calvarium was achieved through dura mater elevation by implants after 4 and 8 weeks in a calvarial rabbit model. Evaluation of the quantity and quality of the NB formation around the two implant surfaces was also assessed in this experiment. We elucidated that spontaneous vertical bone formation could be induced after elevation of the dura mater and the sputtered HA coating significantly enhanced bone formation in a rabbit calvarial model.

In the region below the calvaria where the dura mater was purposely elevated by the two implants, cascade-like NB formation was clearly observed around each implant as well as in the space in between the implants. Furthermore, this NB formation was consistent at 4 and 8 weeks. More noticeably, the ability to promote vertical bone formation without the assistance of any scaffold materials was regularly observed in this study. As shown by the results, the space elevated by the implants was almost completely occupied by newly formed bone that had crept into the implant serrations, starting from the OB down to the end of the implants. This might suggest that the newly formed bone was likely due to the osteoinductive potential from the basal bone surface. This finding is in accordance with the descriptions made in previous studies demonstrating spontaneous NB formation after sinus membrane elevation or periosteal distraction in animals.[1,2,5,6,9,11] Furthermore, connective tissue was rarely observed in this region which might indicate that this calvaria model is more favorable in testing implant surface characteristics compared with the region above the calvaria bone where connective tissue was frequently infiltrated.[37]

In addition, the topography of the implants may be of crucial importance for vertical bone formation. Numerous previous studies have reported that topography of the substrata could influence the proliferation and differentiation of osteogenic cells.[38–40] In this study, serrated implants

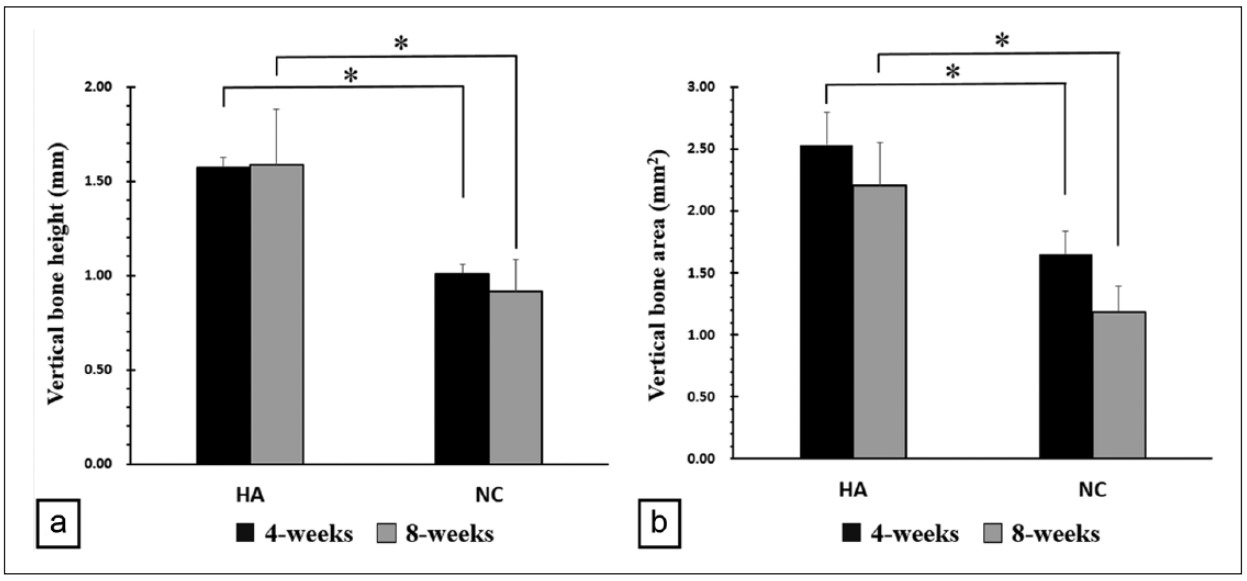

Figure 6. Newly formed bone height and area: (a) vertical bone height below the calvarial bone at 4 and 8 weeks and (b) vertical bone area after 4 and 8 weeks.
HA: HA-coated implant; NC: non-coated implant.
*$p < 0.05$.

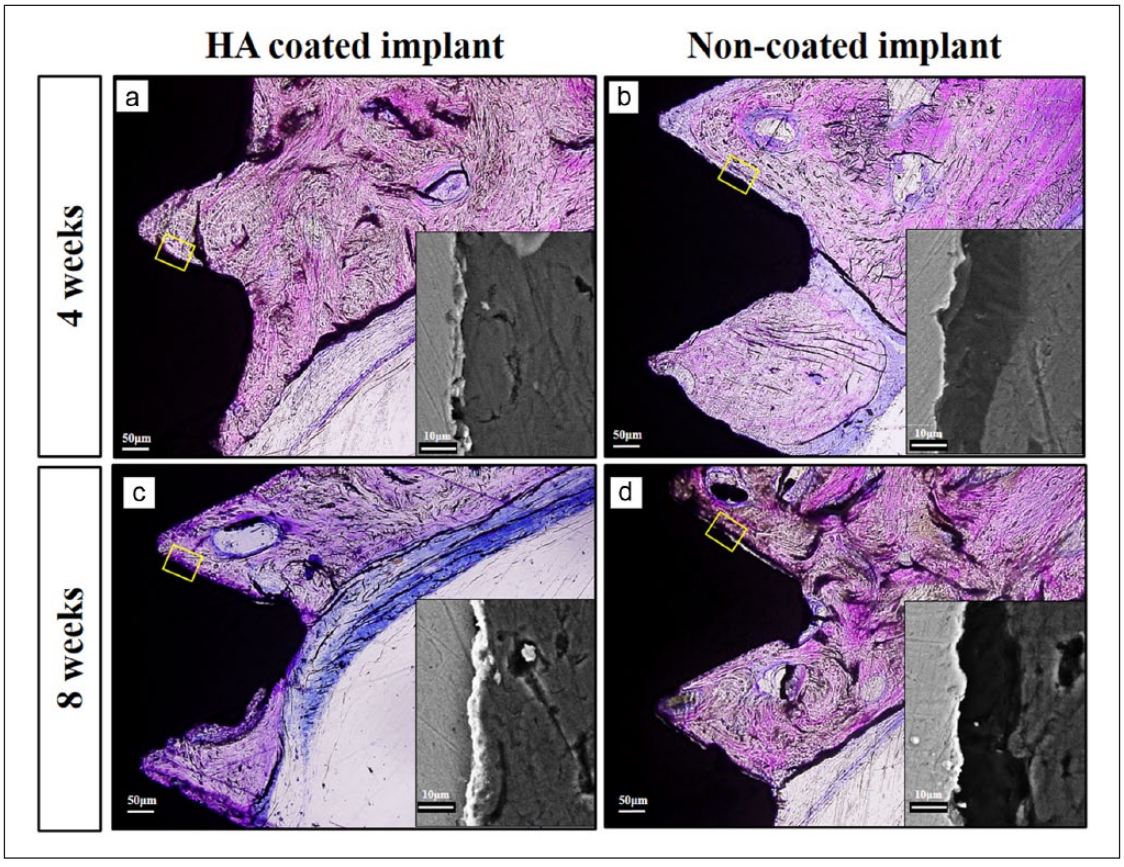

Figure 7. Newly formed bone–implant contact assessed histologically and by SEM after 4 and 8 weeks. Intimate new vertical bone–implant contact in the HA-coated implant group was observed; however, a micro-gap was often detected in the non-coated implant group. (a and c) New bone–implant contact below the calvarial bone in the HA-coated implant after 4 and 8 weeks and (b and d) new bone–implant contact below the calvarial bone in the non-coated implant group after 4 and 8 weeks.
Scale bar in histological images = 50 μm; scale bar in SEM images = 10 μm.

were placed 3 mm under the calvarial bone, so could be regarded as the "bioreactors" that facilitate osteogenic function and further induce vertical bone formation on to the HA-coated and NC implants.

Furthermore, significant vertical bone formation on the HA-coated implant group was observed at both 4 and 8 weeks and VBH around the implants reached up to 1.57 ± 0.06 and 1.58 ± 0.30 mm, respectively. No significant change in bone height at these two time points likely demonstrates that the NB formation induced by the HA-coated implant after dura mater elevation was relatively stable, in contrast to previous studies.[7,37,41,42] Furthermore, this occurs despite the NB formation in this study not being exposed to any form of mechanical stimulation. In previous studies, the range of VBH achieved has been between 0.5 and 1.87 mm with use of additional biomaterials or scaffolds.[7,42,43] The fact that comparable vertical bone formation could be obtained using HA-coated implants after elevation of the dura mater without the need for additional compounds or materials is of particular interest. The HA-coated implant may have osteoinductive capacity by supplying localized calcium and phosphate ions after placement of the implant for the deposition of vertical bone formation. Furthermore, the dura mater, which was displaced downward by the implants, might potentially maintain the ions within the space.

Scanning electron micrographs showed that in the region of NB formation in the HA groups, dense bone was observed between the material and NB interface and solid integration was formed without the presence of microgaps. However, the NC implant presented with microgaps and the distinction between the two implant surfaces was clearly observed. This finding is in consensus with a previous study.[37] The bioactive surface chemistry of the HA coating might play an important role in forming the tight bonding between the coated implants and the newly formed bone. Calcium and phosphate ions released from the HA coating could in effect raise the concentration and deposit biological apatite onto the surface of the implant, which could in turn enhance osteogenic attachment and growth.[43–45] Additionally, the sputtered HA coating used in this study was at ultra-thin thickness. This ultra-thin coating could further enlarge the area and preserve the roughness of the underlying implant surface, which might be more favorable for osteoblastic differentiation and function.[33,46,47]

Importantly, the osteogenic potency of the dura mater in immature animals has been shown to be enhanced compared with that of mature animals.[3,21,22] In this study, all animals were immature, and therefore further studies should also be carried out on mature animals. Additionally, in some samples the dura mater was perforated by the implant, which might have affected the results. Consequently, modifications to the tip of the implant should be considered to avoid this problem reoccurring. Although the model used in this study is unlikely to be directly applied clinically, this is a positive step toward clinical application of this technique following the progression of further research modifications.

Conclusion

This study indicated that vertical bone formation could be induced by dura mater elevation. Furthermore, the resulting bone formation could be significantly enhanced in the presence of HA coating.

Declaration of conflicting interests

The authors declare that there is no conflict of interest.

Funding

This research received no specific grant from any funding agency in the public, commercial, or not-for-profit sectors.

References

1. Zakaria O, Madi M and Kasugai S. A novel osteogenesis technique: the expansible guided bone regeneration. *J Tissue Eng* 2012; 3: 2041731412441194.
2. Schmidt BL, Kung L, Jones C, et al. Induced osteogenesis by periosteal distraction. *J Oral Maxillofac Surg* 2002; 60: 1170–1175.
3. Gosain AK, Santoro TD, Song LS, et al. Osteogenesis in calvarial defects: contribution of the dura, the pericranium, and the surrounding bone in adult versus infant animals. *Plast Reconstr Surg* 2003; 112: 515–527.
4. Evans CH, Palmer GD, Pascher A, et al. Facilitated endogenous repair: making tissue engineering simple, practical, and economical. *Tissue Eng* 2007; 13: 1987–1993.
5. Zakaria O, Kon K and Kasugai S. Evaluation of a biodegradable novel periosteal distractor. *J Biomed Mater Res B Appl Biomater* 2012; 100: 882–889.
6. Zakaria O, Madi M and Kasugai S. Induced osteogenesis using a new periosteal distractor. *J Oral Maxillofac Surg* 2012; 70: e225–e234.
7. Kammerer PW, Palarie V, Schiegnitz E, et al. Vertical osteoconductivity and early bone formation of titanium-zirconium and titanium implants in a subperiosteal rabbit animal model. *Clin Oral Implants Res* 2014; 25: 774–780.
8. Schiegnitz E, Palarie V, Nacu V, et al. Vertical osteoconductive characteristics of titanium implants with calcium-phosphate-coated surfaces—a pilot study in rabbits. *Clin Implant Dent R* 2014; 16: 194–201.
9. Lundgren S, Andersson S, Gualini F, et al. Bone reformation with sinus membrane elevation: a new surgical technique for maxillary sinus floor augmentation. *Clin Implant Dent R* 2004; 6: 165–173.
10. Palma VC, Magro-Filho O, de Oliveria JA, et al. Bone reformation and implant integration following maxillary sinus membrane elevation: an experimental study in primates. *Clin Implant Dent R* 2006; 8: 11–24.
11. Jungner M, Cricchio G, Salata LA, et al. On the early mechanisms of bone formation after maxillary sinus membrane

elevation: an experimental histological and immunohistochemical study. *Clin Implant Dent R*. Epub ahead of print 14 March 2014. DOI: 10.1111/cid.12218.
12. Kusumoto Y, Tachikawa N, Munakata M, et al. Lateral bone window closing technique with poly-l-lactic acid (PLLA) membrane in the augmentation of the maxillary sinus without grafting material: evaluation of bone healing in a rabbit model. *Clin Implant Dent R*. Epub ahead of print 14 April 2015. DOI: 10.1111/cid.12293.
13. Kemp WJ 3rd, Tubbs RS and Cohen-Gadol AA. The innervation of the cranial dura mater: neurosurgical case correlates and a review of the literature. *World Neurosurg* 2012; 78: 505–510.
14. Opperman LA, Passarelli RW, Morgan EP, et al. Cranial sutures require tissue interactions with dura mater to resist osseous obliteration in vitro. *J Bone Miner Res* 1995; 10: 1978–1987.
15. Bradley JP, Levine JP, Roth DA, et al. Studies in cranial suture biology: IV. Temporal sequence of posterior frontal cranial suture fusion in the mouse. *Plast Reconstr Surg* 1996; 98: 1039–1045.
16. Yu JC, McClintock JS, Gannon F, et al. Regional differences of dura osteoinduction: squamous dura induces osteogenesis, sutural dura induces chondrogenesis and osteogenesis. *Plast Reconstr Surg* 1997; 100: 23–31.
17. Greenwald JA, Mehrara BJ, Spector JA, et al. Biomolecular mechanisms of calvarial bone induction: immature versus mature dura mater. *Plast Reconstr Surg* 2000; 105: 1382–1392.
18. MacIsaac ZM, Levine BA, Smith DM, et al. Novel animal model of calvarial defect: part IV. Reconstruction of a calvarial wound complicated by durectomy. *Plast Reconstr Surg* 2013; 131: 512e–519e.
19. Yang Z and Guo Z. A three-dimensional digital atlas of the dura mater based on human head MRI. *Brain Res* 2015; 1602: 160–167.
20. Cooper GM, Durham EL, Cray JJ Jr, et al. Tissue interactions between craniosynostotic dura mater and bone. *J Craniofac Surg* 2012; 23: 919–924.
21. Levi B, Nelson ER, Li S, et al. Dura mater stimulates human adipose-derived stromal cells to undergo bone formation in mouse calvarial defects. *Stem Cells* 2011; 29: 1241–1255.
22. Gosain AK, Gosain SA, Sweeney WM, et al. Regulation of osteogenesis and survival within bone grafts to the calvaria: the effect of the dura versus the pericranium. *Plast Reconstr Surg* 2011; 128: 85–94.
23. Wan DC, Aalami OO, Wang Z, et al. Differential gene expression between juvenile and adult dura mater: a window into what genes play a role in the regeneration of membranous bone. *Plast Reconstr Surg* 2006; 118: 851–861.
24. Reid CA, McCarthy JG and Kolber AB. A study of regeneration in parietal bone defects in rabbits. *Plast Reconstr Surg* 1981; 67: 591–596.
25. Ozcelik D, Turan T, Kabukcuoglu F, et al. Bone induction capacity of the periosteum and neonatal dura in the setting of the rat zygomatic arch fracture model. *Arch Facial Plast Surg* 2003; 5: 301–308.
26. Mabbutt LW, Kokich VG, Moffett BC, et al. Subtotal neonatal calvariectomy. A radiographic and histological evaluation of calvarial and sutural redevelopment in rabbits. *J Neurosurg* 1979; 51: 691–696.
27. Palarie V, Bicer C, Lehmann KM, et al. Early outcome of an implant system with a resorbable adhesive calcium-phosphate coating—a prospective clinical study in partially dentate patients. *Clin Oral Investig* 2012; 16: 1039–1048.
28. Ozeki K, Okuyama Y, Fukui Y, et al. Bone response to titanium implants coated with thin sputtered HA film subject to hydrothermal treatment and implanted in the canine mandible. *Biomed Mater Eng* 2006; 16: 243–251.
29. Zhu X, Son DW, Ong JL, et al. Characterization of hydrothermally treated anodic oxides containing Ca and P on titanium. *J Mater Sci Mater Med* 2003; 14: 629–634.
30. Narayanan R, Seshadri SK, Kwon TY, et al. Calcium phosphate-based coatings on titanium and its alloys. *J Biomed Mater Res B Appl Biomater* 2008; 85: 279–299.
31. Kuwabara A, Hori N, Sawada T, et al. Enhanced biological responses of a hydroxyapatite/TiO2 hybrid structure when surface electric charge is controlled using radiofrequency sputtering. *Dent Mater J* 2012; 31: 368–376.
32. Massaro C, Baker MA, Cosentino F, et al. Surface and biological evaluation of hydroxyapatite-based coatings on titanium deposited by different techniques. *J Biomed Mater Res* 2001; 58: 651–657.
33. Hao J, Kuroda S, Ohya K, et al. Enhanced osteoblast and osteoclast responses to a thin film sputtered hydroxyapatite coating. *J Mater Sci Mater Med* 2011; 22: 1489–1499.
34. Madi M, Zakaria O, Kasugai S, et al. Uncoated implants: bone defect configurations after progressive peri-implantitis in dogs. *J Oral Implantol* 2014; 40: 661–669.
35. Yokota S, Nishiwaki N, Ueda K, et al. Evaluation of thin amorphous calcium phosphate coatings on titanium dental implants deposited using magnetron sputtering. *Implant Dent* 2014; 23: 343–350.
36. Ozeki K, Mishima A, Yuhta T, et al. Bone bonding strength of sputtered hydroxyapatite films subjected to a low temperature hydrothermal treatment. *Biomed Mater Eng* 2003; 13: 451–463.
37. Wang X, Zakaria O, Madi M, et al. Vertical bone augmentation induced by ultrathin hydroxyapatite sputtered coated mini titanium implants in a rabbit calvaria model. *J Biomed Mater Res B Appl Biomater* Epub ahead of print 23 December 2014. DOI: 10.1002/jbm.b.33347.
38. Discher DE, Janmey P and Wang YL. Tissue cells feel and respond to the stiffness of their substrate. *Science* 2005; 310: 1139–1143.
39. Buxboim A and Discher DE. Stem cells feel the difference. *Nat Methods* 2010; 7: 695–697.
40. Ripamonti U, Roden LC and Renton LF. Osteoinductive hydroxyapatite-coated titanium implants. *Biomaterials* 2012; 33: 3813–3823.
41. Kammerer PW, Palarie V, Schiegnitz E, et al. Influence of a collagen membrane and recombinant platelet-derived growth factor on vertical bone augmentation in implant-fixed deproteinized bovine bone–animal pilot study. *Clin Oral Implants Res* 2013; 24: 1222–1230.
42. Draenert FG, Kammerer PW, Palarie V, et al. Vertical bone augmentation with simultaneous dental implantation using crestal biomaterial rings: a rabbit animal study. *Clin Implant Dent R* 2012; 14(Suppl. 1): e169–e174.

43. Le Guehennec L, Soueidan A, Layrolle P, et al. Surface treatments of titanium dental implants for rapid osseointegration. *Dent Mater* 2007; 23: 844–854.
44. Daculsi G, Laboux O, Malard O, et al. Current state of the art of biphasic calcium phosphate bioceramics. *J Mater Sci Mater Med* 2003; 14: 195–200.
45. Davies JE. Understanding peri-implant endosseous healing. *J Dent Educ* 2003; 67: 932–949.
46. Madi M, Zakaria O, Noritake K, et al. Peri-implantitis progression around thin sputtered hydroxyapatite-coated implants: clinical and radiographic evaluation in dogs. *Int J Oral Maxillofac Implants* 2013; 28: 701–709.
47. Mohammadi S, Esposito M, Hall J, et al. Short-term bone response to titanium implants coated with thin radiofrequent magnetron-sputtered hydroxyapatite in rabbits. *Clin Implant Dent R* 2003; 5: 241–253.